Simulation of Intrinsic Defects and Cd Site Occupation in $LaIn_3$ and $LuIn_3$

M. O. Zacate[1,a*], J. P. Bevington[2,b] and G. S. Collins[2,c]

[1]Northern Kentucky University, Highland Heights, KY 41001, USA

[2]Washington State University, Pullman, WA 99164 USA

[a]zacatem1@nku.edu, [b]jbev85@gmail.com, [c]collins@wsu.edu

Keywords: $L1_2$ crystal structure, Cu_3Au crystal structure, diffusion mechanism, solute site occupation

Abstract. In previous work, perturbed angular correlation spectroscopy (PAC) was used to determine jump rates of ^{111}Cd, the daughter of the ^{111}In radiotracer, in the series of phases $R\text{In}_3$ (R = rare-earth element) through nuclear quadrupole relaxation. Greater relaxation, indicating faster Cd jump rates, was observed in heavy rare-earths for compositions more deficient in indium, as would be expected for diffusion mediated by vacancies on the In sublattice. On the other hand, greater relaxation was observed for light rare-earths (R = La, Ce, and Pr) for compositions with excess indium, suggesting Cd diffusion is mediated there by a different mechanism. In this work, computer simulations were carried out to better understand the nature of the relaxation observed for the light rare-earths and the origin of the change in behavior across the rare-earth series. As a first step, formation enthalpies of intrinsic defects were calculated using density functional theory (DFT) for series end-members $LaIn_3$ and $LuIn_3$. Both compounds were found to exhibit Schottky thermal disorder. Additional DFT simulations show that the binding enthalpy between In- and R-vacancies is larger in $LaIn_3$ than in $LuIn_3$, suggesting that diffusion in $LaIn_3$ might be mediated by divacancies. Site enthalpies of Cd also were calculated, and it was found more favorable energetically for Cd to occupy the In sublattice than the R sublattice in both end-member phases.

Introduction

Rare earth tri-indides ($R\text{In}_3$ where R = rare earth element) form in the $L1_2$ crystal structure, shown in Fig. 1. In this structure, indium is coordinated by 4 R sites and 8 In sites, so it is reasonable to expect that tracers on the indium sublattice will diffuse via an indium vacancy mechanism, undergoing first-neighbor jumps without an increase in configurational energy [1]. In such a case, the tracer jump rate w would be given by the formula $w = Z[\text{v}_{\text{In}}]w_2$, where Z=8 is the number of first-neighbor In sites, $[\text{v}_{\text{In}}]$ denotes the fractional indium vacancy concentration, and w_2 is the tracer-vacancy exchange frequency. The corresponding diffusion coefficient would be given by

$$D = \frac{1}{12} f a^2 w \tag{1}$$

where f is the correlation coefficient and a is the lattice parameter. Thus, in the case of an indium vacancy mechanism, the tracer jump rate and the tracer diffusivity will increase as indium vacancy concentration increases as would be the case, for example, for sample compositions with growing indium deficiency.

Using perturbed angular correlation spectroscopy (PAC), cadmium jump rates were determined by measuring nuclear relaxation at opposing phase-boundary compositions in $R\text{In}_3$ across the rare earth series [2]. In heavy rare-earth compounds, cadmium tracers experienced larger relaxation (corresponding to faster jump rates) at indium-poorer compositions, as expected for an indium vacancy diffusion mechanism; however, in the light rare-earth compounds, tracers were found to

have larger relaxation at indium-richer compositions. A decisive composition dependence was not observed for the intermediate rare-earths Nd and Sm.

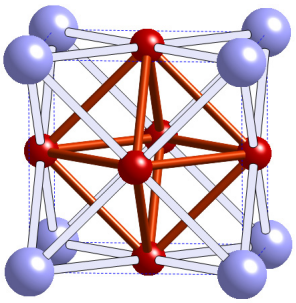

Fig. 1. The $L1_2$ crystal structure. Rare earth atoms are shown as larger spheres and indium as smaller spheres. First neighbors are connected by bars.

As pointed out when larger relaxation was first observed at the indium-richer composition in $LaIn_3$ [3], it is possible to explain the "backwards" composition dependence if cadmium diffuses via a more complex diffusion mechanism such as via a La-vacancy-mediated 6-jump cycle or a divacancy mechanism. For example, if the dominant mode of disorder in $LaIn_3$ involves lanthanum vacancies and La-antisite defects, analogous to triple-defect disorder in $B2$ compounds, then it could be that the indium vacancy concentration is small enough that diffusion of indium and tracers on its sublattice would be mitigated by the lanthanum vacancies. Since lanthanum vacancy concentration is larger at indium-richer compositions, this would explain the composition dependence of nuclear relaxation observed for cadmium in $LaIn_3$.

Diffusion mediated by lanthanum vacancies may not entirely explain the anomalously high cadmium jump rates inferred by relaxation measurements at indium-rich compositions in the light rare earth tri-indides [4]. It has been suggested that the measured relaxation is due at least in part to cadmium shifting off the indium sublattice [4,5], which would happen, for example, if the site occupation energy of cadmium were lower on a rare-earth site than the indium site. The cadmium tracers used in earlier experiments were radioactive daughters of the ^{111}In PAC isotope, and therefore are known to occupy the indium sublattice initially. It is possible that cadmium moves off the indium sublattice shortly after its formation and that this leads to a larger nuclear relaxation than would be observed if cadmium were jumping only among indium lattice sites.

Given the incomplete picture about cadmium movement in $LaIn_3$ and other light rare-earth tri-indides, it is of interest to use computer simulations to help understand the difference in cadmium behavior in the light and heavy rare-earth compounds and to help elucidate the origin of the larger relaxation rates at indium richer compositions in the light rare-earth tri-indides. The first step in such simulations is to determine equilibrium intrinsic defect and cadmium site-occupation properties in representative compounds. This paper presents findings for endmembers of the series: $LaIn_3$ and $LuIn_3$. Implications of these results for interpreting the difference in cadmium jump-rate trends as inferred by hyperfine relaxation measurements in these two compounds will be discussed.

Method

Intrinsic defect and solute site occupation concentrations can be calculated through application of an appropriate thermodynamic model. In this work, the Gibbs free energy of the defective crystal is minimized subject to structural and compositional constraints within the framework of the canonical ensemble. Changes in enthalpy in the thermodynamic model are calculated using density functional theory (DFT).

Consider the general compound $R_{1+4x}In_{3-4x}$ where x denotes deviation from stoichiometric composition RIn_3, and, again, R represents a rare-earth element: La or Lu, in this study. The usual assumption is made that interactions among defects are negligible. In PAC studies using the ^{111}In isotope, tracer mole fraction is on the order of 10^{-12}, which is much smaller than the total concentration of intrinsic defects. Accordingly, in this thermodynamic model, tracer concentration

will be taken to be small enough to be considered negligible in the composition constraint. This gives, as the composition constraint:

$$4x + [\mathrm{In}_R] + \left(\tfrac{3}{4} - x\right)[\mathrm{v}_R] = 3[R_{\mathrm{In}}] + 3\left(\tfrac{1}{4} + x\right)[\mathrm{v}_{\mathrm{In}}], \tag{2}$$

where square brackets are used to denote the fractional concentration of defect on the sublattice specified by the subscript.

Minimization of the Gibbs free energy leads to four equations involving intrinsic defect concentrations. Alternatively, these equations can be obtained by applying the Law of Mass Action to pseudo-chemical disorder reactions that represent defect formation. The reactions and corresponding Mass-Action equations are given in Table 1. They represent Schottky disorder, antisite disorder, and two modes of disorder that are analogous to triple-defect disorder in the *B*2 compounds: called 7-defect and 5-defect in this work.

Table 1. Equilibrium equations and corresponding intrinsic disorder reactions for $R\mathrm{In}_3$.

Equation of equilibrium	Disorder reaction	
$[\mathrm{v}_R][\mathrm{v}_{\mathrm{In}}]^3 = K_{\mathrm{S}} = \exp(-G_{\mathrm{S}}/k_{\mathrm{B}}T)$	$\emptyset \xrightarrow{G_S} \mathrm{v}_R + 3\mathrm{v}_{\mathrm{In}}$	(Schottky)
$\dfrac{[\mathrm{In}_R][R_{\mathrm{In}}]}{[R_R][\mathrm{In}_{\mathrm{In}}]} = K_{\mathrm{AS}} = \exp(-G_{\mathrm{AS}}/k_{\mathrm{B}}T)$	$R_R + \mathrm{In}_{\mathrm{In}} \xrightarrow{G_{AS}} \mathrm{In}_R + R_{\mathrm{In}}$	(Antisite)
$\dfrac{[\mathrm{v}_R]^4[R_{\mathrm{In}}]^3}{[R_R]^3} = K_7 = \exp(-G_7/k_{\mathrm{B}}T)$	$3R_R \xrightarrow{G_7} 4\mathrm{v}_R + 3R_{\mathrm{In}}$	(7-defect)
$\dfrac{[v_{\mathrm{In}}]^4[\mathrm{In}_R]}{[\mathrm{In}_{\mathrm{In}}]} = K_5 = \exp(-G_5/k_{\mathrm{B}}T)$	$\mathrm{In}_{\mathrm{In}} \xrightarrow{G_5} 4\mathrm{v}_{\mathrm{In}} + \mathrm{In}_R$	(5-defect)

Minimization of the Gibbs free energy also leads to equations relating concentrations of cadmium on each sublattice to intrinsic defect concentrations. These equations along with corresponding pseudo-chemical reactions describing the transfer of cadmium from one sublattice to another are given in Table 2.

Table 2. Equilibrium equations and transfer reactions for Cd site occupation in $R\mathrm{In}_3$.

Equation of equilibrium	Transfer reaction
$\dfrac{[\mathrm{Cd}_R][R_{\mathrm{In}}]}{[\mathrm{Cd}_{\mathrm{In}}][R_R]} = K_{\mathrm{x1}} = \exp(-G_{\mathrm{x1}}/k_{\mathrm{B}}T)$	$\mathrm{Cd}_{\mathrm{In}} + R_R \xrightarrow{G_{x1}} \mathrm{Cd}_R + R_{\mathrm{In}}$
$\dfrac{[\mathrm{Cd}_R][\mathrm{v}_{\mathrm{In}}]}{[\mathrm{Cd}_{\mathrm{In}}][\mathrm{v}_R]} = K_{\mathrm{x2}} = \exp(-G_{\mathrm{x2}}/k_{\mathrm{B}}T)$	$\mathrm{Cd}_{\mathrm{In}} + \mathrm{v}_R \xrightarrow{G_{x2}} \mathrm{Cd}_R + \mathrm{v}_{\mathrm{In}}$
$\dfrac{[\mathrm{Cd}_R][\mathrm{In}_{\mathrm{In}}]}{[\mathrm{Cd}_{\mathrm{In}}][\mathrm{In}_R]} = K_{\mathrm{x3}} = \exp(-G_{\mathrm{x3}}/k_{\mathrm{B}}T)$	$\mathrm{Cd}_{\mathrm{In}} + \mathrm{In}_R \xrightarrow{G_{x2}} \mathrm{Cd}_R + \mathrm{In}_{\mathrm{In}}$

As shown below, only three equations in Table 1 are independent, and only one equation in Table 2 is needed to determine equilibrium cadmium site occupation. Thus, if three of the free energies of disorder, G_{S}, G_{AS}, G_7 and G_5, and one of the free energies of transfer, $G_{\mathrm{x}n}$, are known, the defect concentrations can be calculated by solving numerically the systems of equations given

by three equations in Table 1, one equation in Table 2, Eq. 2, and two additional relations to eliminate [R_R] and [$\mathrm{In_{In}}$]:

$$[\mathrm{In_{In}}] = 1 - [R_{\mathrm{In}}] - [\mathrm{v_{In}}] \text{ and } [R_R] = 1 - [\mathrm{In}_R] - [\mathrm{v}_R], \tag{3}$$

again under the assumption that [Cd_R] and [$\mathrm{Cd_{In}}$] are much smaller than the dominant intrinsic defect concentrations.

Thus, determination of defect concentrations and Cd site occupation depends only on values of free energies of disorder and of solute transfer. They can be expressed in terms of what have been called defect formation energies, denoted in the present work by $\left(g_Y^X\right)^f$ for defect X on sublattice Y, and by the formation energy per formula unit of the perfect lattice, $g^f_{R\mathrm{In}_3}$. In this notation, $G_{\mathrm{S}} = \left(g_R^{\mathrm{v}}\right)^f + 3\left(g_{\mathrm{In}}^{\mathrm{v}}\right)^f + g^f_{R\mathrm{In}_3}$, $G_{\mathrm{AS}} = \left(g_R^{\mathrm{In}}\right)^f + \left(g_{\mathrm{In}}^R\right)^f$, $G_7 = 4\left(g_R^{\mathrm{v}}\right)^f + 3\left(g_{\mathrm{In}}^R\right)^f + g^f_{R\mathrm{In}_3}$, $G_5 = 4\left(g_{\mathrm{In}}^{\mathrm{v}}\right)^f + \left(g_R^{\mathrm{In}}\right)^f + g^f_{R\mathrm{In}_3}$, $G_{\mathrm{x1}} = \left(g_R^{\mathrm{Cd}}\right)^f + \left(g_{\mathrm{In}}^R\right)^f - \left(g_{\mathrm{In}}^{\mathrm{Cd}}\right)^f$, $G_{\mathrm{x2}} = \left(g_R^{\mathrm{Cd}}\right)^f + \left(g_{\mathrm{In}}^{\mathrm{v}}\right)^f - \left(g_{\mathrm{In}}^{\mathrm{Cd}}\right)^f - \left(g_R^{\mathrm{v}}\right)^f$, and $G_{\mathrm{x3}} = \left(g_R^{\mathrm{Cd}}\right)^f - \left(g_{\mathrm{In}}^{\mathrm{Cd}}\right)^f - \left(g_R^{\mathrm{In}}\right)^f$. Note that $4G_{\mathrm{S}} + 3G_{\mathrm{AS}} = G_7 + 3G_5$, so that only three disorder reactions are needed to specify intrinsic disorder completely. Only one transfer reaction is needed, because reaction energies of various transfer reactions differ only by intrinsic disorder energies: $G_{\mathrm{x3}} = G_{\mathrm{x1}} - G_{\mathrm{AS}} = G_{\mathrm{x2}} + G_{\mathrm{S}} - G_5$.

The defect formation energy corresponds to the change in energy required to move the non-defect atom out of site Y in the crystal to a reference state, which often is taken to be a pure metal of substance Y, and to move a defect of species X from a reference state into the vacant lattice site in the crystal. That is, $\left(g_Y^X\right)^f = g_Y^X(N) - Ng^0_{R\mathrm{In}_3} + g_Y^0 - g_X^0$ where N indicates the number of atoms in the crystal, $g^0_{R\mathrm{In}_3}$ is the energy per atom of the perfect crystal so that $Ng^0_{R\mathrm{In}_3}$ is the energy of the perfect crystal with N atoms, $g_Y^X(N)$ is the energy of an equivalent size crystal with defect X_Y, and g_X^0 and g_Y^0 are the energy per atom of X and Y in their reference states. For X = vacancy, g_X^0 is zero. The formation energy of $R\mathrm{In}_3$ is given by the difference in energy of $R\mathrm{In}_3$ and the energies of R and In in their reference states; that is, $g^f_{R\mathrm{In}_3} = 4g^0_{R\mathrm{In}_3} - g_R^0 - 3g_{\mathrm{In}}^0$.

It is noteworthy that reference-state energies g_X^0 cancel when calculating disorder-reaction and transfer energies, so that reaction and transfer energies may be determined without calculating energies of pure metals or other reference conditions. In that case, $G_{\mathrm{S}} = g_R^{\mathrm{v}} + 4g^0_{R\mathrm{In}_3}$, $G_{\mathrm{AS}} = g_R^{\mathrm{In}} + g_{\mathrm{In}}^R$, $G_7 = 4g_R^{\mathrm{v}} + 3g_{\mathrm{In}}^R + 4g^0_{R\mathrm{In}_3}$, $G_5 = 4g_{\mathrm{In}}^{\mathrm{v}} + g_R^{\mathrm{In}} + 4g^0_{R\mathrm{In}_3}$, $G_{\mathrm{x1}} = g_R^{\mathrm{Cd}} + g_{\mathrm{In}}^R - g_{\mathrm{In}}^{\mathrm{Cd}}$, $G_{\mathrm{x2}} = g_R^{\mathrm{Cd}} + g_{\mathrm{In}}^{\mathrm{v}} - g_{\mathrm{In}}^{\mathrm{Cd}} - g_R^{\mathrm{v}}$, and $G_{\mathrm{x3}} = g_R^{\mathrm{Cd}} - g_{\mathrm{In}}^{\mathrm{Cd}} - g_R^{\mathrm{In}}$. Here g_Y^X, which is sometimes called the raw defect energy [6], denotes the difference in energy of the crystal with and without the defect: $g_Y^X = g_Y^X(N) - Ng^0_{R\mathrm{In}_3}$ for an N-atom crystal.

Above, free energies, G and g, can be expressed in terms of corresponding enthalpies and vibrational entropies: $G = H - TS_{\mathrm{vib}}$ and $g = h - Ts_{\mathrm{vib}}$. Often, vibrational contributions to the free energy are not considered when using computer simulations to perform an initial characterization of a material's defect properties, and that is true for the present analysis.

In this work, defect enthalpies h_Y^X and the enthalpy per atom of $R\mathrm{In}_3$, $h^0_{R\mathrm{In}_3}$, were calculated within the framework of density functional theory (DFT) using the LAPW/dAPW basis set [7] as implemented in the WIEN2k code [8]. That is, full-potential linearized augmented plane-waves

with additional local-orbital basis functions (LAPW+LO) [9] were used for valence and semi-core electrons in s- and p-states while augmented plane waves with local orbitals (APW+lo) [7,10] were used for d- and f-states. The Perdew-Burke-Ernzerhof generalized gradient approximation (GGA) [11] was used as the exchange-correlation functional, and calculations were carried out without spin polarization. Atom-specific parameters (muffin-tin sphere radii and local orbitals) were as follows: R_{MT} = 2.50 a.u. with a 4d lo for In; R_{MT} = 2.50 a.u. with a 4p LO for Cd; R_{MT} = 2.50 a.u. with 6s and 5p LOs for La; and R_{MT} = 2.50 a.u. with 6s and 5p LOs for Lu. Basis set sizes were determined using $R_{MT}K_{max}$ = 9.5, spherical harmonics inside atomic spheres were expanded up to maximum angular momentum l_{max} = 10, and the charge density was expanded up to G_{max} = 12 a.u.$^{-1}$.

Calculations were carried out on supercells containing N = 32 atoms constructed from 2×2×2 unit cells under constant pressure; *i.e.*, the lattice parameter was adjusted to minimize enthalpy at zero pressure. Defect calculations were full relaxed; that is, atomic coordinates of all 32 atoms (or 31 for vacancy calculations) were adjusted to minimize enthalpy independent of symmetry constraints. The tetrahedron method [12] was used to perform integrations in reciprocal space by sampling 63 k points in the reduced first Brillouin zone of the supercell. Calculations were run to self-consistency with an energy convergence criterion of 0.01 mRy, and atomic-coordinate relaxation calculations were run until forces on atoms were less than 0.2 mRy/bohr.

Results

Calculated enthalpy per atom of RIn$_3$ and defect enthalpies are given in Table 3. Corresponding disorder formation enthalpies, transfer enthalpy for the second transfer reaction, and vacancy-vacancy association enthalpy (introduced below) are given in Table 4.

Table 3. Defect enthalpies and enthalpy per atom of RIn$_3$. All quantities in eV.

Quantity	R = La (LaIn$_3$)	R = Lu (LuIn$_3$)
$h^0_{R\mathrm{In}_3}$	-177,878.444	-219,263.302
h^{v}_{R}	231,236.062	396,774.819
$h^{\mathrm{v}}_{\mathrm{In}}$	160,094.135	160,093.587
h^{In}_{R}	71,145.549	236,685.692
h^{R}_{In}	-71,137.524	-236,677.105
h^{Cd}_{R}	78,960.508	244,499.714
$h^{\mathrm{Cd}}_{\mathrm{In}}$	7,817.5794	7,817.325
$h^{\mathrm{v:v}}_{\mathrm{In}:R}$	391,329.996	556,868.436

Table 4. Disorder enthalpies, transfer reaction 2 enthalpy, and vacancy association enthalpy.

Quantity	R = La (LaIn$_3$)	R = Lu (LuIn$_3$)
H_S [eV/defect]	1.173	0.594
H_{AS} [eV/defect]	4.012	4.293
H_7 [eV/defect]	2.557	2.107
H_5 [eV/defect]	1.663	1.367
H_{x2} [eV]	1.002	1.157
H_A [eV]	-0.201	0.030

As can be seen in Table 4, the Schottky disorder enthalpy-per-defect has the smallest value of all modes of disorder in each compound, indicating that vacancies will have much larger concentrations than antisite defects. This can be verified readily by calculating defect concentrations at, for example 600 K, taking vibrational entropies to be zero for simplicity, and graphing as a function of composition, as in Fig. 2. These results differ significantly from earlier calculations [13], which determined the lowest-enthalpy mode of disorder in $LaIn_3$ to be the 5-defect defect and the antisite and 7-defect modes to be nearly equivalent in $LuIn_3$. In the earlier calculations, disorder formation enthalpies were calculated under the condition of constant volume. The present results are favored, as constant pressure better represents experimental conditions.

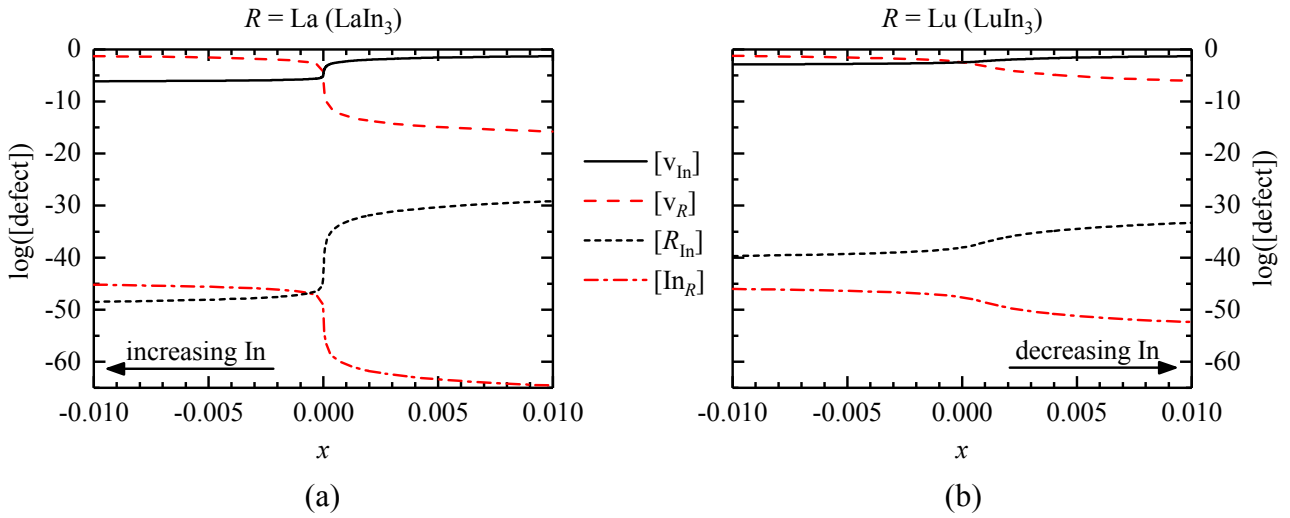

Fig. 2. Log plots of intrsinic defect conncentraions as a function of deviation from stoichiometry x at 600 K for disorder enthlapies reported in Table 4 and assuming disorder entropies are zero for (a) $La_{1+4x}In_{3-4x}$ and for (b) $Lu_{1+4x}In_{3-4x}$.

Given that vacancies have the largest concentrations in these compounds, transfer reaction x2 provides the most direct equation for determining cadmium site occupation. Values obtained are given in Table 4. They indicate that it is energetically unfavorable for cadmium to switch from an indium site to a rare-earth site in both $LaIn_3$ and $LuIn_3$.

Since vacancies are predicted to be the dominant intrinsic defects in these compounds, it is of interest to consider whether or not rare-earth and indium vacancies experience an attractive interaction. A vacancy-vacancy interaction can be considered using the pseudo-chemical reaction for vacancy association:

$$\mathrm{v}_R + \mathrm{v}_{\mathrm{In}} \xrightarrow{G_{\mathrm{A}}} \{\mathrm{v}_R : \mathrm{v}_{\mathrm{In}}\}, \tag{4}$$

where a negative association energy G_{A} indicates an attractive interaction. It can be expressed in terms of defect energies as $G_{\mathrm{A}} = g^{\mathrm{v:v}}_{\mathrm{In}:R} - g^{\mathrm{v}}_{R} - g^{\mathrm{v}}_{\mathrm{In}}$ where $g^{\mathrm{v:v}}_{\mathrm{In}:R}$ denotes the difference in energy in the crystal with v_R and v_{In} defects in first neighbor positions and in the crystal with no defects; that is, $g^{\mathrm{v:v}}_{\mathrm{In}:R} = g^{\mathrm{v:v}}_{\mathrm{In}:R}(N) - Ng^{0}_{R\mathrm{In}_3}$. Again, N is the number of atoms in the crystal, or, in the case of a defect calculation, the number of atoms in the simulation supercell. The corresponding enthalpies, $h^{\mathrm{v:v}}_{\mathrm{In}:R}$, calculated using DFT are given Table 3. The association energies H_{A} are reported in Table 4. As can be seen, an attractive interaction between indium and lanthanum vacancies is predicted whereas indium and lutetium vacancies are predicted to be very weakly repulsive.

Discussion

Schottky disorder is found more commonly in insulating and semiconducting compounds than in intermetallic compounds. It is, therefore, interesting that Schottky disorder is the lowest mode of disorder in $LaIn_3$ and $LuIn_3$. Although one may reasonably expect that $LaIn_3$ and $LuIn_3$, as endmembers of the series, would be representative of the whole series, calculation of disorder formation enthalpies in the other rare-earth tri-indides likely would be of value to confirm that vacancies are indeed the dominant defects in all the rare-earth tri-indides.

The lower Schottky disorder enthalpy in $LuIn_3$ indicates that concentrations of vacancies will be higher in $LuIn_3$ than $LaIn_3$. If the Schottky disorder enthalpy decreases monotonically across the rare earth series, then one would expect to find larger vacancy concentrations as one shifts toward heavier rare earth elements. This, in turn, would result in increasing tracer jump rates (and increasing nuclear relaxation) toward the heavier rare earths, as was observed in the heavy rare-earth tri-indides using PAC [2]. It does not, on the other hand, explain the reverse trend observed in the light-rare earths: that nuclear relaxation increases when moving toward the lighter rare-earth element. This suggests that a different physical process is responsible for the nuclear relaxation.

Given that v_{In} is one of the dominant defects in $LaIn_3$, as predicted by these calculations, it is difficult to understand how a v_{La}-mediated 6-jump cycle mechanism or anti-structure-bridge mechanism would lead to a larger diffusion rate for Cd on the In sublattice. Therefore, on the basis of the present calculations of equilibrium defect concentrations, diffusion mechanisms driven by v_{La} defects appear to be unlikely explanations for the large nuclear relaxation observed at the indium-rich composition in $LaIn_3$. The difference in vacancy association behavior in $LaIn_3$ and $LuIn_3$ is intriguing, suggesting that a divacancy mechanism could explain elevated Cd jump rates at indium-richer compositions in $LaIn_3$.

Following the reasoning of Kurita and Koiwa [14], one can define 12 associated v_{In}-v_R-pair-midpoints per unit cell. Identifying these midpoints as pair "lattice sites," then the vacancy-pair concentration can be defined as $[v_R : v_{In}] \equiv N^{v:v}_{In:R} / N_p$ where $N^{v:v}_{In:R}$ denotes the number of vacancy pairs and N_p denotes the total number of pair lattice sites in the crystal. Noting that the proportion of these pair-sites to In sites to rare-earth sites is 12:3:1 and approximating $[In_R]$ and $[R_{In}]$ as zero in accord with the negligible antisite concentrations predicted by the disorder enthalpies in Table 4, Eqs. 3 can be written

$$[In_{In}] = 1 - [v_{In}] - 4[v_R : v_{In}] \text{ and } [R_R] = 1 - [v_R] - 12[v_R : v_{In}]. \quad (5)$$

Application of the Law of Mass Action for the association reaction in Eq. 4 gives

$$\frac{[v_R : v_{In}]}{[v_R][v_{In}]} = K_A = \exp(-G_A / k_B T). \quad (6)$$

And, inclusion of $[v_R : v_{In}]$ in Eq. 2 while neglecting the antisite concentrations gives a new equation of constraint:

$$4x + \left(\tfrac{3}{4} - x\right)[v_R] + 6(1 - 4x)[v_R : v_{In}] = 3\left(\tfrac{1}{4} + x\right)[v_{In}]. \quad (7)$$

Numerical solution of the Schottky equilibrium equation and Eqs. 5-7 gives concentrations of vacancies and the vacancy-pair. Fig. 3 shows these concentrations as a function of composition at 600 K for the Schottky disorder enthalpy calculated for $LaIn_3$ for four different association enthalpies. As can be seen, for sufficiently negative association enthalpy, the vacancy-pair concentration will exceed the indium vacancy concentration for certain ranges of indium-rich compositions (x<0). This is best illustrated for the -0.8 eV association enthalpy. If migration

barriers are comparable for the simple v_{In} diffusion mechanism and for the divancancy mechanism, then one would expect diffusion of tracers to be governed by the v_{In} mechanism near x=0 where [v_{In}] exceeds [v_R:v_{In}] and by the divacancy mechanism for x<0 where [v_R:v_{In}] exceeds [v_{In}].

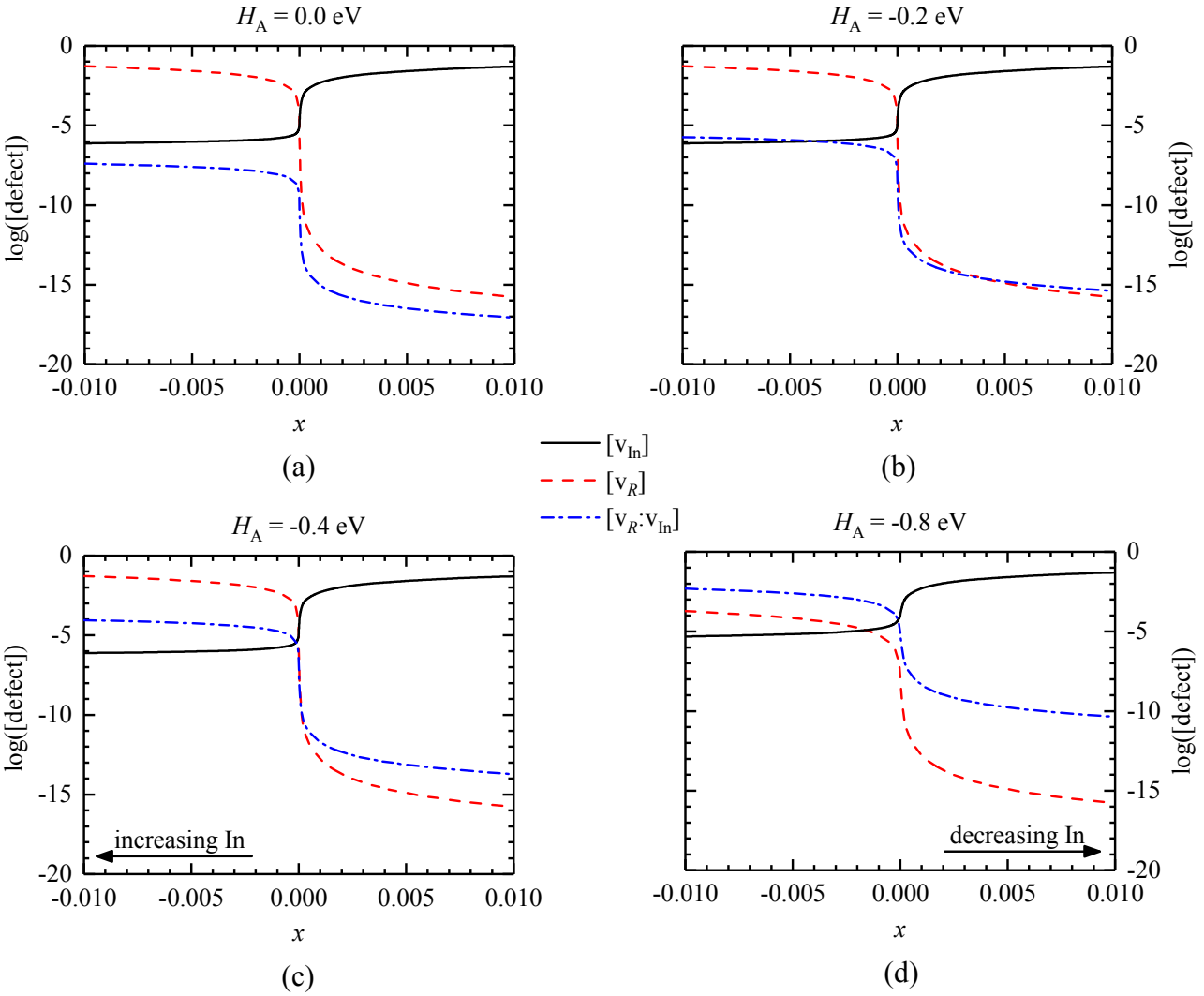

Fig. 3. Log plots of vacancy and vacancy-pair concentrations in $La_{1+4x}In_{3-4x}$ as a function of x at 600 K for the disorder enthalpies reported in Table 4 and for selected values of vacancy-vacancy association enthalpy: (a) 0 eV, (b) -0.2 eV, (c) -0.4 eV, and (d) -0.8 eV. In all graphs, entropies were taken to be zero.

According to the calculations of the present work, the association enthalpy in $LaIn_3$ is only -0.20 eV. As can be seen in Fig. 3b, [v_R:v_{In}] only marginally exceeds [v_{In}] at large deviation from stoichiometry at 600 K, and this result alone cannot explain the large difference in nuclear relaxation observed for cadmium at the phase boundaries of $LaIn_3$. Additional calculations are needed to draw a definitive conclusion regarding the possibility that diffusion of Cd is mediated by the divacancy defect for indium richer compositions in $LaIn_3$. (1) The 2×2×2 supercell may be small enough that defect images influence calculated enthalpies, so this should be investigated by repeating defect enthalpy calculations using a 3×3×3 supercell. This may yield an association enthalpy that is more negative. (2) Nonzero entropies could enhance (or diminish) [v_R:v_{In}], so phonon frequencies should be calculated to determine vibrational contributions to the free energy significantly impacts [v_R:v_{In}]. (3) Even without a significant change in [v_R:v_{In}] due to inclusion of vibrational effects, it could be that the divacancy mechanism provides a lower effective migration

barrier for Cd tracers; therefore, migration barriers for the indium-vacancy and the divacancy mechanisms should be calculated to see if the divacancy barrier is lower. (4) For completeness, migration barriers for other competing diffusion mechanisms should be calculated to verify that they are not lower than those of the vacancy and the divacancy mechanisms. DFT-based calculations of migration barriers for competing diffusion mechanisms have been performed to investigate other $L1_2$ compounds [15,16,17].

With regards to the hypothesis that the increased nuclear relaxation observed for cadmium at indium richer compositions in $LaIn_3$ is due to a shift of cadmium off the indium sublattice [4], the large transfer enthalpy calculated for reaction 2 strongly indicates it is unlikely that the cadmium shifts to the lanthanum sublattice. It does not, however, rule out the possibility that cadmium on a lanthanum site is stabilized when bound with an intrinsic defect or that cadmium shifts to an interstitial position. Additional calculations with these other defect configurations need to be performed in order to evaluate further the cadmium site-switching possibility.

Summary

As the first step in a study of cadmium movement in the series of rare-earth tri-indies using computer simulation, density functional theory was used to calculate defect formation and cadmium site-occupation enthalpies in $LaIn_3$ and $LuIn_3$, which allowed prediction of equilibrium defect concentrations using a thermodynamic model. Key findings were as follows.

1) Schottky disorder is the lowest enthalpy mode in $LaIn_3$ and $LuIn_3$, indicating that indium vacancies and rare-earth vacancies have much larger concentrations than antisite defects.
2) There is a modestly attractive interaction between indium vacancies and lanthanum vacancies, but there is a weakly repulsive interaction between indium and lutetium vacancies
3) It is energetically unfavorable for Cd to occupy the rare-earth sublattice in both $LaIn_3$ and $LuIn_3$.

The vacancy-interaction result suggests that diffusion at the indium-rich boundary of $LaIn_3$ might be mediated by divacancies, which could explain why cadmium was found to experience a larger nuclear relaxation, corresponding to a higher jump rate, at the indium-rich boundary. These calculations do not fully explain why the jump rates inferred by nuclear relaxation measurements at the indium-rich boundary in $LaIn_3$ are anomalously high, but they do indicate it is unlikely that the large relaxation is caused by a shift of cadmium from the indium to the lanthanum sublattice. The calculations do not rule out the possibility that cadmium moves to an interstitial lattice location [4]. Additional calculations are needed to determine effects of simulation size and lattice vibrations, migration barriers of candidate diffusion mechanisms, and enthalpies of cadmium in interstitial sites in order to develop a fuller understanding of cadmium movement in the rare earth tri-indides.

Acknowledgement

This work has been supported through the National Science Foundation under grants DMR 09-04096, DMR 15-08189, and DMR 18-09531.

References

1. Y.M. Young, E.W. Elcock, Monte Carlo studies of vacancy migration in binary ordered alloys: I, Proc. Phys. Soc. 89 (1966) 735-746.

2. G.S. Collins, X. Jiang, J.P. Bevington, F. Selim, M.O. Zacate, Change of diffusion mechanism with lattice parameter in the series of lanthanide indides having $L1_2$ structure, Phys. Rev. Lett. 102 (2009) 155901.
3. M.O. Zacate, A. Favrot, and G.S. Collins, Atom Movement in In_3La Studied Via Nuclear Quadrupole Relaxation, Phys. Rev. Lett. 92 (2004) 225901; Erratum, Phys. Rev. Lett. 93 (2004) 49903.
4. G.S. Collins, Atom motion in solids following nuclear transformation, Defect and Diffusion Forum (this volume).
5. G.S. Collins, Diffusion and Equilibration of Site-Preferences Following Transmutation of Tracer Atoms, Diffusion Foundations 19 (2019) 61-79.
6. Y. Mishin, Chr. Herzig, Diffusion in the Ti-Al system, Acta Mater. 48 (2000) 589-623.
7. G.K.H. Madsen, P. Blaha, K. Schwarz, E. Sjöstedt, L. Nordström, Efficient linearization of the augmented plane-wave method, Phys. Rev. B 64 (2001) 195134.
8. P. Blaha, K. Schwarz, G. Madsen, D. Kvasnicka, and J. Luitz, WIEN2k, An Augmented Plane Wave Plus Local Orbitals Program for Calculating Crystal Properties, Karlheinz Schwarz, Technical Universität Wien, Austria, 2001.
9. D. Singh, Ground-state properties of lanthanum: Treatment of extended-core states, Phys. Rev. B 43 (1991) 6388.
10. E. Sjöstedt, L. Nordström, D.J. Singh, An alternative way of linearizing the augmented plane-wave method, Solid State Commun. 114 (2000) 15.
11. J. P. Perdew, K. Burke, M. Ernzerhof, Generalized gradient approximation made simple, Phys. Rev. Lett. **77**, 3865 (1996).
12. P. E. Blöchl, O. Jepsen, O. K. Anderson, Improved tetrahedron method for Brillouin-zone integrations, Phys. Rev. B 49, 16223 (1994).
13. J.P. Bevington, Lattice locations and diffusion in intermetallic compounds explored through PAC measurements and DFT calculations, PhD Dissertation, Washington State University (2011).
14. N. Kurita, M. Koiwa, Correlation factor in diffusion in the $L1_2$ structure for atomic migration via triple defects, Intermetallics 10 (2002) 735-741.
15. P. Gopal, S.G. Srinivasan, First-principles study of self- and solute diffusion mechanisms in γ'-Ni_3Al, Phys. Rev. B 86 (2012) 014112.
16. T.-T. Shi, J.-N. Wang, H.-C. Wang, B.-Y. Tang, Atomic diffusion mediated by vacancy defects in pure and transition element (TM)-doped (TM = Ti, Y, Zr, or Hf) $L1_2$ Al_3Sc, Materials and Design 108 (216) 529-537.
17. S. Liu, Z. Li, C. Wang, First-principles study of solute diffusion in Ni_3Al, Chin. Phys. B 26 (2017) 093102.